DEVELOPMENT AND APPLICATIONS OF A TWO-PARAMETER COHESION FUNCTION FOR CUBIC EQUATIONS OF STATE

Sylvana Derjani-Bayeh, Freddy L. Figueira and Claudio Olivera-Fuentes*

Grupo TADiP, Departamento de Termodinámica y Fenómenos de Transferencia
Universidad Simón Bolívar, AP89000, Caracas 1080, Venezuela

E-mail: claudio@usb.ve

Abstract. The Stamateris–Olivera–Figueira (SOF) cohesion function is based on the behavior of the configurational internal energy, rather than on the repulsion-attraction interpretation of cubic equations of state. It contains two adjustable parameters for each component, and can take negative values at supercritical temperatures. In this paper, we review the work done in development and implementation of the SOF function, and present some new applications for nonpolar and polar fluid mixtures. We conclude that the SOF cohesion function performs generally as well as, and in many cases better than, other cohesion functions usually employed with cubic equations of state.

Keywords: Equation of state, cubic, cohesion function, supercritical, phase equilibria

1. Introduction

Despite considerable advances in the development of theoretically based equation of state (EOS) models, engineering practice still relies heavily on simpler, semi-empirical cubic EOSs of the Van der Waals type, especially 2P1T cubic EOSs, thus called because they contain two substance-specific ("2P") parameters, only one of which ("1T") depends on temperature [1]. These EOSs have the general form

$$P = \frac{RT}{v-b} - \frac{a(T)}{v^2 + k_1 b v + k_2 b^2} \tag{1}$$

where a is the attraction parameter, and b is the covolume parameter. Both parameters are usually derived from the critical properties of the fluid as

$$a(T) = \Omega_{ac} \frac{R^2 T_c^2}{P_c} \alpha(T_r) \quad , \quad b = \Omega_b \frac{RT_c}{P_c} \tag{2}$$

In Equation (1), constants k_1 and k_2 define a particular "family" of 2P1T cubic EOSs, the best known being the Van der Waals (VW, $k_1 = k_2 = 0$), Redlich–Kwong (RK, $k_1 = 1$, $k_2 = 0$), and Peng–Robinson (PR, $k_1 = 2$, $k_2 = -1$) lineages. Their values in turn determine the family-specific constants Ω_{ac} and Ω_b in Eq. (2). A central element is the cohesion or alpha function $\alpha(T_r)$ in Equation (2), defined as

$$\alpha(T_r) \equiv \frac{a(T)}{a(T_c)} \simeq \frac{a}{a_c} \quad \square \quad \alpha(1) \equiv 1 \tag{3}$$

A large variety of alpha functions have been proposed through the years. Van der Waals originally took a as a constant [2], but later realized that a temperature dependence was required in order to improve EOS performance [3]. Early attempts involved universal functions of reduced temperature, but the modern stage of development was reached only after Wilson [4] and most notably Soave [5] showed that the alpha function could be fitted to vapor pressure data of each pure fluid. The Wilson and Soave (S72) forms are, respectively

$$\alpha(T_r) = T_r\left[1 + m\left(\frac{1}{T_r} - 1\right)\right] \tag{4}$$

$$\alpha(T_r) = \left[1 + m\left(1 - T_r^{\frac{1}{2}}\right)\right]^2 \tag{5}$$

The main drawback of this standard tuning of cubic EOS is that saturation data exist only up to the critical temperature. Use of the EOS at supercritical conditions therefore involves an extrapolation that will largely depend on the mathematical form of the alpha function. As an example, Figure 1(a) is a plot of □ of the RK EOS for methane, computed from saturation data obtained from the NIST Webbook [6] and fitted with Equations (4) and (5), evaluating m at the "omega temperature" Tr = 0.7, i.e. from the acentric factor □. Both functions give very similar results in the range of experimental data, yet predict entirely different behaviors above the critical temperature. Since Equation (4) gives a constant derivative d□/dTr, □ decrease monotonically with increasing temperature until it eventually goes to negative values. By contrast, Equation (5) precludes the possibility of negative □, which reaches a minimum value (zero) and increases thereaf with temperature. Also included in Figure 1(a) is the curve generated by the alpha function developed by Twu et al. (TW) [7], which goes asymptotically to zero at infinite temperature,

$$\alpha = T_r^{N(M-1)} exp[L(1 - T_r^{NM}] \tag{6}$$

A traditional interpretation of Equation (1) is that the two terms on the rhs represent repulsive and attractive contributions to fluid pressure, in that order. Based on this reading, it is frequently affirmed that α should not take negative values, because they are physically meaningless. However, in van der Waals generalized molecular theory, the equation of state is obtained only as [8-10]

$$P = NkT\left(\frac{\partial ln V_f}{\partial V}\right)_{T,N} - \frac{N}{2}\left(\frac{\partial \Phi}{\partial V}\right)_{T,N} \tag{7}$$

where V_f is the "free volume" that excludes the hard-core (HC) region around each molecular center, where other molecules cannot be present, and Φ is the average longer-distance potential that contains not just attraction effects, but also soft repulsions. Although the second term on the rhs of Equation (7) must vanish identically at infinite temperature, it may be positive at high (but finite) temperatures, where P is slightly greater than P^{HC} because of soft repulsions [10]. More importantly, the assumptions that lead from Equation (7) to Equation (1) are questionable at best. Even van der Waals himself [3] was aware of the deficiencies of his "repulsion" term, which is based on the formula $V_f = V–b$ with constant excluded volume b and gives only a first-order approximation to the equation of state of hard spheres [11]. General expressions are not available either for the temperature and density dependencies of the "attraction" term [8, 9]. No theoretical significance can therefore be ascribed to the parameters in Equation (1); the practical success of 2P1T cubic EOS hinges on a fortunate compensation of errors, aided by empirical adjustments of the second term, even though the hard-core term is more in need of improvement [11].

Experimental evidence strongly suggests that α can and should take negative values at supercritical temperatures [3, 12–15]. Colina et al. [16] remarked that the analysis of sub- and supercritical cohesion data, and in particular their extrapolation to infinite temperature, was made simpler by representing the ratio α/T_r as a function of reduced reciprocal temperature or "coldness" $1/T_r$. These authors obtained supercritical values of α by four different methods:

a) From saturation pressures, fitted and extrapolated with a quadratic extension of Equation (4) equivalent to a proposal by Soave (S79) [17],
b) From pressures on the critical isochore,
c) From second virial coefficients,

$$B_R \overset{\text{def}}{\equiv} \frac{BP_c}{RT_c} = \Omega_b - \Omega_{ac}\frac{\alpha}{T_r} \tag{8}$$

d) From Joule-Thomson inversion curves, by numerical solution of the first order ODE [18]

$$\frac{d\alpha}{dT_r} - c(\theta)\frac{\alpha}{T_r} = d(\theta) \quad , \quad c(\theta) \stackrel{\text{def}}{\equiv} \frac{\theta(2\theta + k_1)}{\theta^2 + k_1\theta + k_2} \quad , \quad d(\theta) \stackrel{\text{def}}{\equiv} -\frac{\Omega_b}{\Omega_{ac}}\frac{\theta^2 + k_1\theta + k_2}{(\theta - 1)^2} \tag{9}$$

where $\theta = v/b$ is a dimensionless volume.

Figure 1(b) is a plot of α/T_r of the RK EOS computed for simple fluids modeled with the Lee-Kesler EOS [19]. Results are shown for subcritical α computed from saturation pressures and supercritical α obtained by the above procedures. Three of the four methods predict negative α at high temperatures. The fact that the various predictions differ from each other only serves to highlight the fallibility of the 2P1T cubic EOS, which is unable to represent all fluid properties with a single formulation. In particular, the negative values obtained from methods b), c) and d) do not arise from any "unphysical" postulated alpha function, but are the direct result of applying the EOS model to different fluid properties.

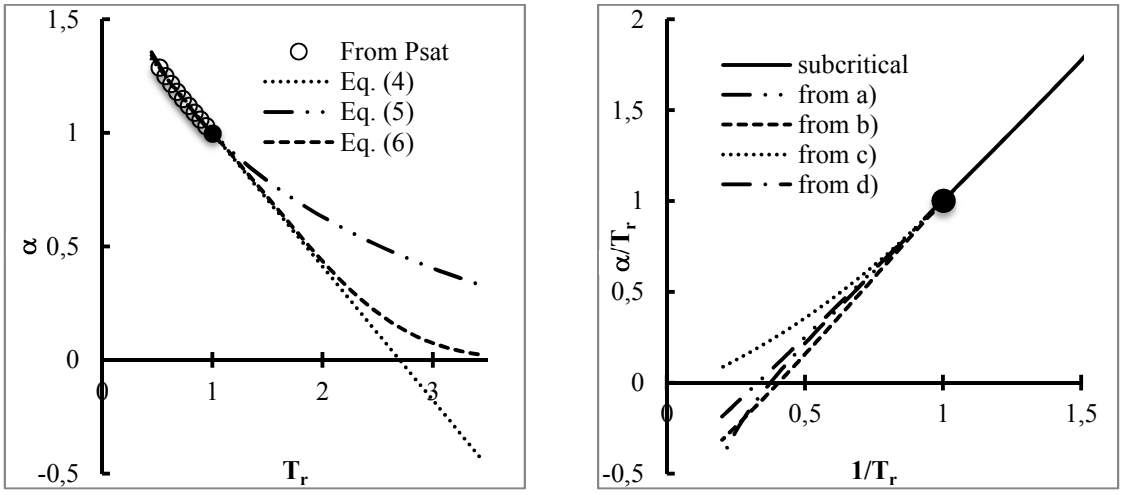

Figure 1. Subcritical and supercritical α for the RK EOS: (a) Extrapolated for methane with three different cohesion functions; (b) Computed for simple fluids with four different methods.

2. Development of the SOF cohesion function

2.1 Formulation and justification

From Equation (1), an expression for the residual internal energy follows as

$$u^{res} = -a_c\beta(T_r)\int_v^\infty \frac{dv}{v^2 + k_1bv + k_2b^2} \tag{10}$$

with β defined as

$$\beta \stackrel{\text{def}}{\equiv} \alpha - T_r\frac{d\alpha}{dT_r} = \frac{d(\alpha/T_r)}{d(1/T_r)} \tag{11}$$

Although Equation (10) derives from Equation (1), there is reason to expect that it may be more successful as a model of the configurational energy of fluids than Equation (1) is as a model of pressure. To start with, the same Equation (10) is obtained if the first term in Equation (1) is replaced by any other function of volume (improving the van der Waals repulsion term, e.g. with a density-dependent b), provided that the temperature dependence is maintained to comply with the ideal gas limit. Furthermore, from molecular theory, the residual energy is associated to soft repulsion and attraction effects, which we have seen is the proper interpretation of the alpha function. Some interesting conclusions may then be obtained. Since the integral in Eq. (10) is positive for all physically meaningful volumes $v > b$, and the residual internal energy is expected

to be negative (because energy must be expended to draw the fluid molecules apart and reach the ideal gas state, hence the alternative name "cohesive energy" given to this residual property), and go to zero at infinite temperature (because only hard-core repulsions remain active in this limit), it follows that β must be positive definite,

$$\beta \geq 0 \quad , \quad \lim_{T_r \to \infty} \beta = 0 \tag{12}$$

Thus, the most that can be concluded about the alpha function is that α/T_r is an increasing function of $1/T_r$. Only a constant α, identical therefore to β, would be subject to the nonnegativity condition, but of course both would equal unity as required by Equation (3). The constraint $a > 0$ might be valid for the original van der Waals EOS, but ceases to be mandatory once a is made temperature dependent.

We call β the cohesive energy or beta function, and consider it as a more fundamental function than α. From its definition, it seems reasonable to express it as a function of reciprocal reduced temperature. The SOF cohesion function [20, 21] is based on the two-parameter ansatz

$$\beta = \frac{m}{T_r^{n-2}} \tag{13}$$

which, by integration with the boundary condition of Equation (3), leads to

$$\frac{\alpha}{T_r} = 1 + \frac{m}{n-1}\left(\frac{1}{T_r^{n-1}} - 1\right) \tag{14}$$

2.2 Pure-component parameters

Using saturation pressure data generated from the DIPPR database [22], optimized values of m and n for use with the VW, RK and PR EOSs were obtained for 846 fluids [21]. Parameter tables are available from the authors. If the above molecular considerations are valid, we should expect from Equation (12) that $m > 0$ and $n > 2$, but we must stress that the optimization was free from any such constraints. We present in Figure 3 a graphical summary of the parameters obtained for the RK and PR EOSs; results for VW are entirely similar. We find in effect that $m > 0$ for all fluids, and $n > 2$ in about 97% of cases. The exceptions correspond to nearly the same substances for the three EOSs, including quantum gases, certain self-associating compounds, glycols and a few other polyfunctional compounds. It is possible that a more complex beta function is required for these compounds. In all cases, however, we see that $n > 1$ showing that u^{res} is at least finite at zero coldness. From Equation (14), the infinite temperature limit of α/T_r will be negative if $m > n - 1$, which is the case for virtually all compounds, with isolated exceptions that appear in Figure 3 as points above the diagonal line $m = n - 1$.

Unlike the single adjustable coefficient in one-parameter cohesion functions such as Equations (4) and (5), the two SOF parameters m and n cannot be computed from a single saturation data point, and should not be expected to depend only on acentric factor. An extended corresponding states correlation was developed using critical compressibility factor Z_c as fourth parameter in addition to ω [21, 23],

$$m = g_0 + g_1 Z_c + g_2 \omega \tag{15}$$

$$\frac{0.7^{1-n} - 1}{n-1} \stackrel{\text{def}}{=} r = \frac{f_0 + f_1 \omega}{m} \tag{16}$$

$$n = \sum_{k=0}^{6} n_k r^k \tag{17}$$

Coefficients for these formulas are given in [21, 23].

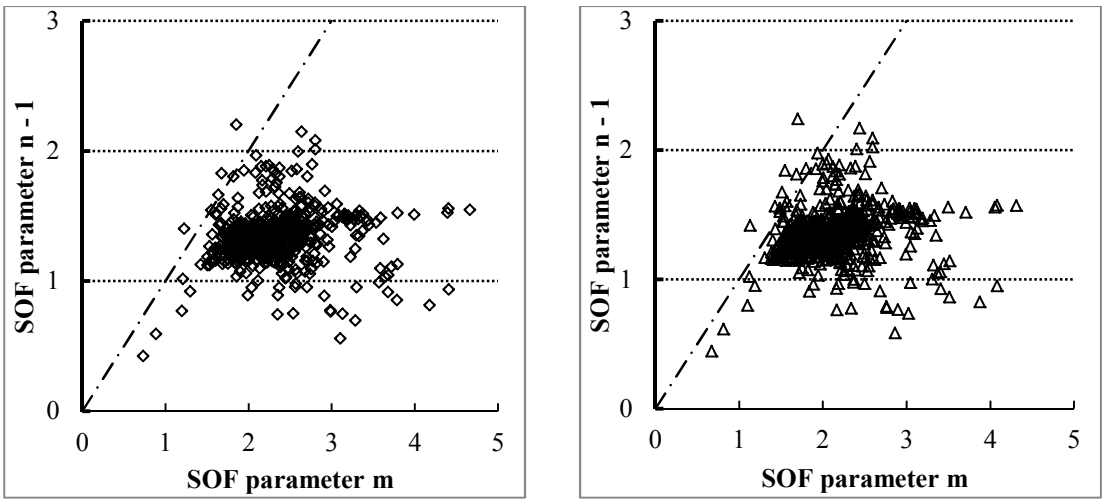

(a) RK EOS (b) PR EOS

Figure 2. SOF parameters for 846 fluids. The diagonal line corresponds to $m = n - 1$.

2.3 Extension to mixtures

Equation (1) can be extended to mixtures by making a and b functions of composition according to the classical van der Waals one-fluid mixing rules,

$$a_m = \sum_i \sum_j x_i x_j a_{ij} \quad , \quad b_m = \sum_i \sum_j x_i x_j b_{ij} \tag{18}$$

where a_{ii}, b_{ii} are the pure-component parameters, and a_{ij}, b_{ij} ($i \neq j$) are the cross coefficients, traditionally estimated from the combining rules

$$a_{ij} = \left(1 - k_{ij}\right)\left(a_{ii} a_{jj}\right)^{1/2} \tag{19}$$

$$b_{ij} = (b_{ii} + b_{jj})/2 \tag{20}$$

where k_{ij} is a binary interaction parameter (BIP). Clearly, the geometric-mean or Berthelot combining rule for a_{ij}, Equation (19), cannot be used if (only) one of the pure-component parameters is negative. Although this has been held as another reason for the unacceptability of negative cohesion parameters [15], the argument can be easily reverted. Theoretical support for Equation (19) is rather tenuous, drawn from the London theory of dispersive forces, where intermolecular cross-attractions between two spherical, nonpolar molecules with similar ionization potentials can be approximated by the geometric-mean average [24]. But if parameter a in Equation (1) does not represent purely attractive forces, Equation (19) ceases to be adequate as a combining rule, as proved by the mere fact that a BIP is needed in practice to compensate for deviations from the theoretical behavior. Actually, there should be no need for any combining rule, because if the BIP must be obtained from experimental data on the binary *i-j* system, the same data can perfectly well be used to find a_{ij} directly, rather than k_{ij}. Aside from this pragmatic approach, it is fairly straightforward to devise variants of Equation (19) consistent with the possibility of negative α. Noting first that it is no longer possible to work with reduced temperatures, we write, from Equations (3), (11) and (13) for each component,

$$\frac{d(a/T)}{d(1/T)} = a_c \beta = \frac{a_c m T_c^{n-2}}{T^{n-2}} = \frac{M}{T^{n-2}} \quad , \quad M \stackrel{\text{def}}{=} a_c m T_c^{n-2} \tag{21}$$

The mixing/combining rules are now applied to obtain the derivative for the mixture,

$$\frac{d(a_m/T)}{d(1/T)} = \sum_i \sum_j x_i x_j (1 - k_{ij}) \left[\frac{M_{ii} M_{jj}}{T^{n_{ii}+n_{jj}-4}}\right]^{1/2} \tag{22}$$

where the double subscript denotes pure component parameters. Integration from $1/T = 0$ yields

$$\frac{a_m}{T} = \left(\frac{a_m}{T}\right)_\infty + \sum_i \sum_j x_i x_j \frac{M_{ij}}{(n_{ij} - 1) T^{n_{ij}-1}} \tag{23}$$

with

$$M_{ij} \overset{\text{def}}{\equiv} (1 - k_{ij}) \left(M_{ii} M_{jj}\right)^{1/2} \quad , \quad n_{ij} \overset{\text{def}}{\equiv} \frac{n_i + n_j}{2} \tag{24}$$

Since $m > 0$ (hence $M > 0$) for all fluids studied, these combination rules can be applied without problem. It would be tempting to set the infinite-temperature limit $(a_m/T)_\infty$ in Equation (23) to zero, but Equation (14) shows that this does not vanish for the pure fluids. Rather, it has the value

$$\left(\frac{a_{ii}}{T}\right)_\infty = \frac{a_{ci}}{T_{ci}} \left(1 - \frac{m_{ii}}{n_{ii} - 1}\right) \tag{25}$$

and would be zero only if the optimal parameters had fallen on the diagonal line in Figure 3, but then of course the cohesion function would have been prevented from taking negative values. The difference between a/T and the above limiting value,

$$\frac{a_{ii}}{T} - \left(\frac{a_{ii}}{T}\right)_\infty = \frac{M_{ii}}{(n_{ii} - 1) T^{n_{ii}-1}} \tag{26}$$

can be interpreted as a corrected attraction parameter that discounts the repulsive contributions missed by the van der Waals repulsion term. This opens up a second way to generate the combining rule. Since the "excess" a/T in Equation (26) is always positive, the mixing/combining rules can be applied as

$$\left[\frac{a_m}{T} - \left(\frac{a_m}{T}\right)_\infty\right] = \sum_i \sum_j x_i x_j (1 - k_{ij}) \left\{\left[\frac{a_{ii}}{T} - \left(\frac{a_{ii}}{T}\right)_\infty\right] \left[\frac{a_{jj}}{T} - \left(\frac{a_{jj}}{T}\right)_\infty\right]\right\}^{1/2} \tag{27}$$

giving

$$\frac{a_m}{T} = \left(\frac{a_m}{T}\right)_\infty + \sum_i \sum_j x_i x_j \frac{M_{ij}}{(n_{ii} n_{jj} - 2 n_{ij} + 1) T^{n_{ij}-1}} \tag{28}$$

with M_{ij}, n_{ij} defined in Equation (24). There is no substantial difference between Equations (23) and (28). A prescription must be found in any case for $(a_m/T)_\infty$, which should be a function of composition that reduces to Equation (25) for the pure components. If this in fact represents a correction for repulsion effects, an arithmetic-mean combining rule might be appropriate, e.g.

$$\left(\frac{a_m}{T}\right)_\infty = \sum_i \sum_j x_i x_j \frac{1 - l_{ij}}{2} \left[\left(\frac{a_{ii}}{T}\right)_\infty + \left(\frac{a_{jj}}{T}\right)_\infty\right] \tag{29}$$

or we might keep the geometric mean combining rule if the pure-component limits are all negative,

$$\left(\frac{a_m}{T}\right)_\infty = \sum_i \sum_j x_i x_j (1 - l_{ij}) \left[\left(\frac{a_{ii}}{T}\right)_\infty \left(\frac{a_{jj}}{T}\right)_\infty\right]^{1/2} \tag{30}$$

In both cases, new BIPs appear that might give added flexibility to Equations (23) and (28). Yet another possibility would be to dispense with combining rules altogether, and adjust the cross parameters at infinite temperature directly from experimental data, as already mentioned. These and other proposals are of course open to study, but the main point is that it is the beta function, not alpha, that truly represents cohesive energy, and should be the target of the mixing/combining rules. Finally, it must be remarked that the fact that Equation (14) allows for negative α does not necessarily mean that such values will arise in every situation. As shown in Figure 1, the alpha function crosses the zero axis at relatively high reduced temperatures. Heavy substances, or light fluids at moderate supercritical conditions, will exhibit positive α and Equation (19) can be still applied, as in several of the applications described below.

3. Applications of the SOF cohesion function

3.1 Saturation properties of pure fluids

Poling et al. [25] included the VW-SOF EOS in their test of the capabilities of several cubic EOSs and cohesion functions to predict saturated volumes, residual properties and fugacities of propane at two specified conditions. Unfortunately, these authors inadvertently used an incorrect form of the SOF function, omitting the T_r denominator in the lhs of Equation (14). This of course gave worse results than other cubic models, so inferior in fact that it is remarkable that the authors did not realize that something was amiss about their computations. When the calculations are redone with the correct version of Equation (14), the VW-, RK- and PR-SOF models give results as good as, or better than, most other EOSs included in the original comparison [21].

We show in Table 1 the average absolute deviation (AAD) of saturation pressures predicted by Equation (14) and three other two-parameter alpha functions proposed by Soave (S79) [17], Gibbons and Laughton (GL) [26], and Stryjek and Vera (SV) [27]. Parameters for these functions were obtained in all cases with the same optimization procedure and for the same set of 846 fluids [28–30]. All four functions are seen to give very similar deviations, with perhaps just a slight edge in favor of Equation (14). A limited comparison using a subset of 56 fluids of interest in petroleum refining (light gases, paraffins up to C20, olefins and aromatics) [31] has also shown that these functions predict enthalpies of vaporization with comparable AADs ranging from 3.4% with Equation (14) to 3.6% with GL. Thus, we may conclude that properly adjusted two-parameter cohesion functions perform essentially the same in predicting fluid properties at saturation conditions in the subcritical region.

Table 1. Percent AAD of saturation pressures of pure fluids predicted with two-parameter cohesion functions

EOS	S79	GL	SV	SOF
VW	2.91	2.55	2.57	2.33
RK	2.94	2.52	2.55	2.33
PR	3.12	2.38	2.47	2.40

3.2 Hydrocarbon mixtures with H_2S and CO_2

Barrios et al. [32, 33] studied the vapor-liquid equilibrium (VLE) of binary systems of H_2S, CO_2 and paraffinic hydrocarbons up to C10. Isothermal P-x-y data were collected from the literature for 23 hydrocarbon binaries, 12 mixtures with CO_2, 7 mixtures with H_2S, and the system CO_2/H_2S. Optimal BIPs were computed by minimizing the fugacity objective function proposed by Paunović et al. [34]. The VW, RK and PR EOSs were combined with the S72, S79, GL, SV, TW and SOF functions, using Equation (19) in all cases, because negative values of α did not arise in the range of experimental temperatures. BIPs for hydrocarbon–hydrocarbon interactions could be set to zero without significant loss of precision (AADs less than 2.0% and 0.3% for pressures and vapor compositions, respectively), but nonzero values were definitely required for systems with either H_2S or CO_2. BIPs were found in general to increase with temperature, strongly so near the critical temperature of the heavier component. They did not change greatly with the choice of cohesion function for a given EOS, indicating once again that all models give similarly good representation of saturation properties. Tables of optimal BIPs are available from the authors. A

corresponding-states correlation was developed for BIPs in terms of reduced temperature and acentric factor of the heavier component (*j*),

$$k_{ij} = k'_{ij}(\omega_j) - \frac{k''_{ij}(\omega)}{|1 - T_{rj}|} \tag{31}$$

with coefficients given in [33]. There is virtually no deterioration in the VLE results using the correlation instead of the optimal BIPs. Figure 3 presents two examples of predicted phase diagrams.

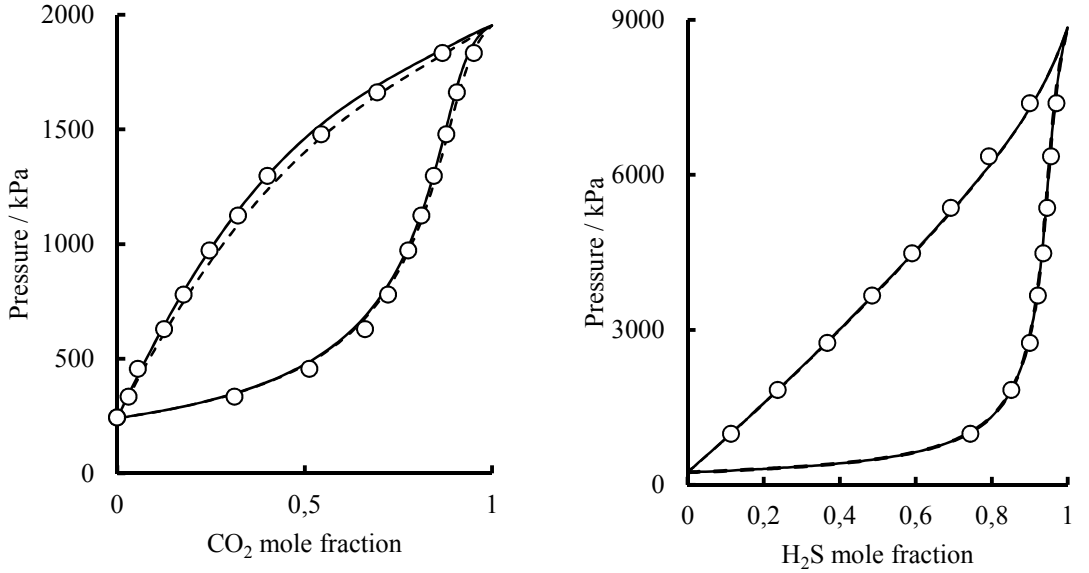

(a) CO_2 – propane at 252.95 K using RK-SOF (b) H_2S – n-hexane at 372.90 K using VW-SOF

Figure 3. VLE predicted using optimal (solid lines) and correlated (dashed lines) BIPs.

We have used the above optimal BIPs and generalized correlations to predict VLE of 12 ternary systems (9 containing only hydrocarbons, 2 containing CO_2, and one containing both CO_2 and H_2S) for which experimental data were available in the literature. Two five-component and one six-component hydrocarbon mixtures were also included. Pressure AADs range from about 4% to 6% using the optimal BIPs, increasing to about 8% when the correlations are used. The lowest deviation is obtained with PR-S79. Composition AADs lie between about 6.0% and 6.5% for all models. Equation (14) places first or second best, with very little difference between results from either optimal or correlated BIPs.

3.3 Distillation curves of petroleum fractions

From Equations (15)–(17), characteristic parameters *m* and *n* can be predicted for substances not in the database, and in particular for ill-defined fluids such as petroleum fractions, if the basic physical data (critical properties and acentric factor) are available or can be estimated by suitable methods. Using the various EOS/alpha function combinations, we have computed distillation curves of 12 light cuts, with API gravities from 31.5 to 74.2, for which data were found in the literature [35]. The experimental ASTM D86 curves were converted into true boiling point (TBP) curves using the correlations of Daubert [36]. Pseudo-components were defined at 10 K intervals, with normal boiling points (NBP) at half interval and specific gravities obtained from the Watson factor of the cut. Critical properties and acentric factor of each pseudo-component were then estimated using correlations by Twu [37]. With the mixture thus characterized, the ASTM D86 distillation was simulated as a sequence of flash separations. We observed however that the assumption of zero BIP between hydrocarbon pairs resulted in large errors, especially at the light end, i.e. at the distillation onset. It was necessary therefore to estimate BIPs for the pseudo-component pairs, and this was done by least-squares minimization of the temperature deviations. We found that BIPs were related to the NBPs in the form

$$k_{ij} = k'_{ij} + \frac{k''_{ij}}{NBP_j - NBP_i} \tag{32}$$

with coefficients given in Table 2. Figure 4(a) shows the simulated distillation curves for Geddes Cut 4 using PR-SOF with zero and non-zero BIPs. The noticeable improvement in the predictions when BIPs are introduced contradicts the widespread assumption of zero BIPs for these mixtures, e.g. in process simulators. A global decrease in deviations was obtained, roughly from 5 K to 1.6 K, very similar for all combinations as shown in the bar chart of Figure 4(b), suggesting that selection of the EOS and cohesion function may not be crucial when the BIPs are fitted to experimental data.

Table 2. Coefficients of Equation (32) for Geddes [35] oil cuts

Nº	Cut type	k_{ij}'	k_{ij}''	Nº	Cut type	k_{ij}'	k_{ij}''
1	Naphtha	-0.062	1.449	7	Catalytic naphtha	-0.003	0.370
2	VM & P naphtha	-0.221	3.881	8	Catalytic naphtha	-0.060	1.453
3	White gasoline	-0.216	4.010	9	Catalytic naphtha	-0.060	1.697
4	Naphtha	-0.153	2.589	10	Light naphtha	-0.008	0.323
5	Unstripped naphtha	-0.117	2.097	11	Light naphtha	-0.007	0.690
6	Unstripped naphtha	-0.152	2.490	12	Heavy naphtha	-0.040	1.096

3.4 Joule-Thomson inversion curves

Joule-Thomson inversion curves (JTIC) provide an extremely sensitive test of the volume and temperature dependencies of any EOS. Equation (9) can be solved for inversion temperatures by assigning values to the dimensionless volume θ, which runs from 1 to infinity. Inversion pressures are then obtained by substitution in Equation (1). We note from Equations (11), (13) and (14) that

$$\frac{d\alpha}{dT_r} = \frac{\alpha - \beta}{T_r} = (2 - n)\frac{\alpha}{T_r} + (n - 1 - m) \tag{33}$$

hence Equation (9) has a direct solution for α/T_r, with T_r following from Equation (14) as

$$T_{r,inv} = \left[1 + \frac{n-1}{m}\left(\frac{d(\theta) + m - n + 1)}{2 - n - c(\theta)} - 1\right)\right]^{1/(1-n)} \tag{34}$$

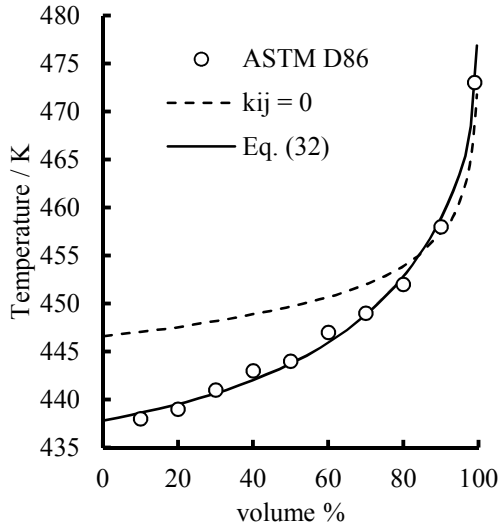

(a) Simulated ASTM D86 distillation of oil cut 4

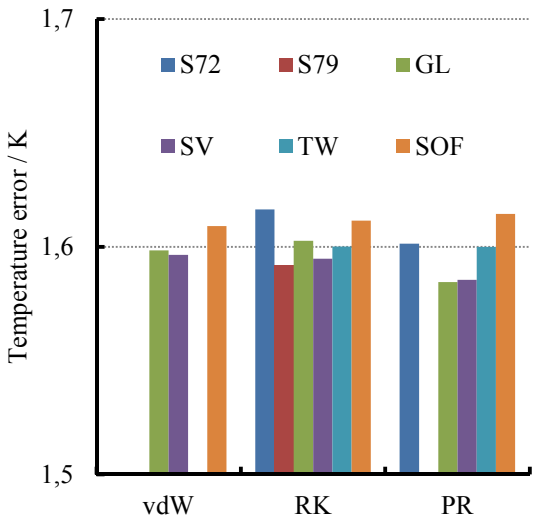

(b) Global errors in simulated ASTM D86 curves

Figure 4. Prediction of distillation curves of ligh oil cuts

We remark that Equation (34) is single-valued, i.e. the SOF function avoids the pitfalls of other well-known cohesion functions that predict more than one inversion curve [38]. An important characteristic point is the terminus of the JTIC in the high-temperature, zero-pressure limit where the fluid approaches ideal gas behavior. Letting $\theta \rightarrow \infty$, $c \rightarrow 2$, $d \rightarrow -\Omega_b/\Omega_{ac}$ we get the maximum inversion temperature as

$$T_{r,inv}^{max} = \left[1 + \frac{n-1}{mn}\left(\frac{\Omega_b}{\Omega_{ac}} - m - 1\right)\right]^{1/(1-n)} \tag{35}$$

a result that can also be established from Equation (8) by imposing the condition

$$\frac{d(B_R/T_r)}{d(1/T_r)} = 0 \quad \square \quad \frac{\alpha + \beta}{T_r} = \frac{\Omega_b}{\Omega_{ac}} \tag{36}$$

Figure 5 is a plot of inversion curves predicted for argon using the VW, RK and PR EOSs with the SOF function. Maximum inversion temperatures are listed in Table 3. Also included for comparison are values obtained from the corresponding-states correlation developed for simple fluids by Gunn et al. [39]. It can be seen that none of these models reproduces the empirical data satisfactorily, as could be expected from Figure 2, where alpha values that match a JTIC differ from those obtained by extrapolation of a subcritical function. In particular, maximum inversion temperatures, and also peak inversion pressures, decrease with increasing ζ_c (0.307… for PR, 0.333… for RK, 0.375 for VW). As discussed in [40], the shape of the predicted JTIC can be adjusted by performing the transformation $v \rightarrow v + t$ where t is the volume translation parameter. As an example, we show in Figure 5 that PR-SOF with $t = -0.009(RT_c/P_c)$ obtained by inspection gives greatly improved results. Similar attempts with the VW and RK EOS, however, are not successful, so that this procedure appears to be of limited utility.

Table 3. Maximum inversion temperatures for argon

Gunn et al. [36]	VW-SOF	RK-SOF	PR-SOF	PR-SOF-tr
5.075	3.738	4.383	5.484	5.234

3.5 Equilibrium of hydrocarbon systems with hydrogen

Special challenges are faced when modelling systems containing hydrogen. The cohesion parameter of this quantum fluid exhibits a maximum at an intermediate subcritical temperature, which cannot be captured with traditional one-parameter functions such as S72.

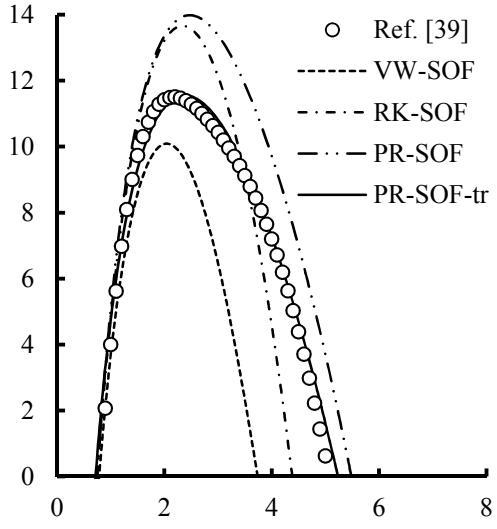

Figure 5. Predicted JTICs for argon

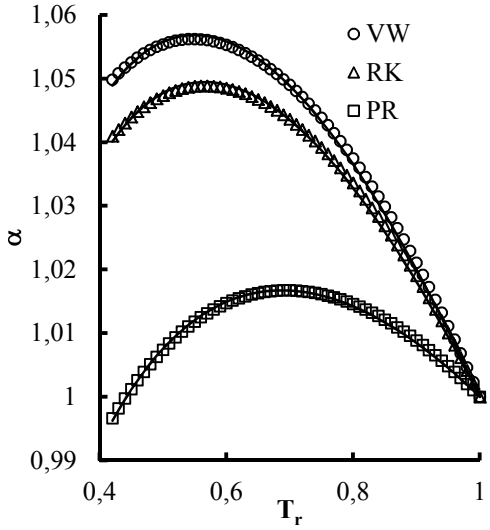

Figure 6. Subcritical α of hydrogen

As shown in Figure 6, the SOF function does an excellent job of reproducing the entire subcritical curve, but of course this is also true of other two-parameter functions such as GL and TW. Secondly, given the very low critical temperature of H_2, there is a very certain possibility that α may become negative at temperatures within the range of practical applications. Preliminary calculations based on critical isochore data generated from the reference equation of Leachman et al. [41] suggest that this may happen somewhere between 150 and 250 K, depending on the EOS. Even if negative values are not attained, the cohesion function will need to be extrapolated well past the critical temperature, and its correct behavior is crucially important.

Bastida et al. [42, 43] studied the VLE of 15 binary mixtures of H_2 with paraffins, olefins and aromatics, and also with CO, CO_2 and Ar. The mixing/combining rules of Equations (23) and (30) were used in three different forms, denoted as (SOF-1C) $l_{ij} = 0$ and constant k_{ij}, (SOF-2C) $l_{ij} \neq 0$ and constant k_{ij}, and (SOF-1T) $l_{ij} = 0$ and temperature-dependent k_{ij}. Optimal BIPs were obtained by minimization of the implicit objective function proposed by Englezos et al. [44]. The pressure (P) and vapor composition (Y) AADs were compared with predictions obtained using BIP correlations developed by Huron et al. [45] and Bosse et al. [46] for the RK and PR EOSs. We summarize the results in Table 4, and present two examples of predicted phase diagrams in Figure 7. It can be seen that the SOF cohesion function, with one temperature-dependent BIP, gives generally better predictions than the other SOF options, and also than other methods recommended in the literature.

Table 4. AADs in the prediction of VLE of hydrogen-containing binary systems

	VW		RK		PR	
	$AAD_{(P)}$	$AAD_{(Y)}$	$AAD_{(P)}$	$AAD_{(Y)}$	$AAD_{(P)}$	$AAD_{(Y)}$
SOF-1C	14.6	2.78	12.4	2.79	14.4	2.29
SOF-2C	30.8	4.62	23.7	3.96	14.7	2.69
SOF-1T	10.5	1.69	11.8	3.23	9.35	1.98
Ref. [45]	-	-	19.8	4.12	18.8	3.88
Ref. [46]	-	-	34.7	4.31	21.4	4.28

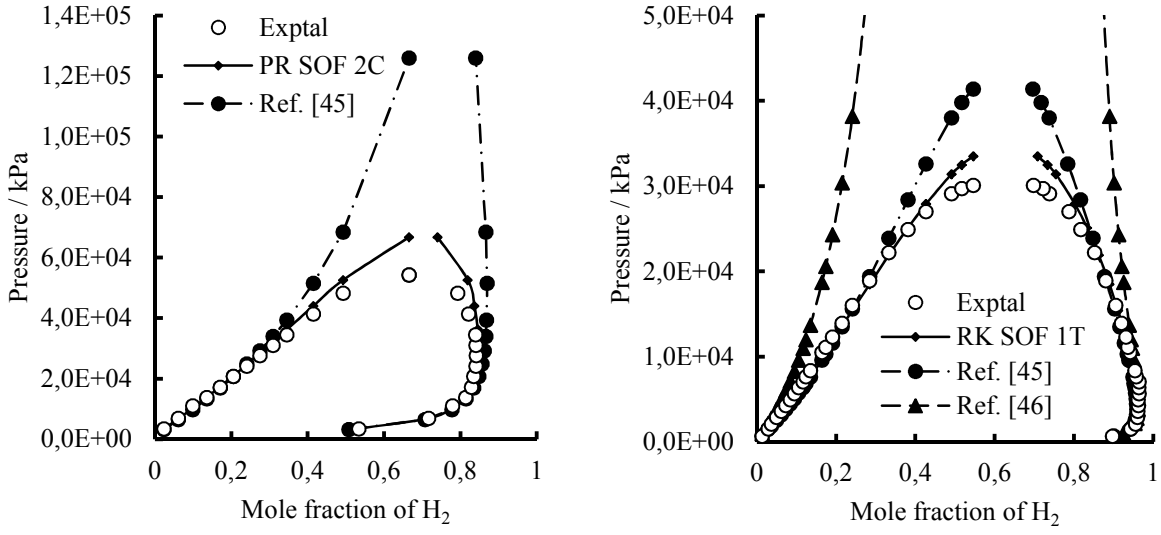

(a) H_2 – propane at 310.92 K (b) H_2 – CO_2 at 77.3 K

Figure 7. Predicted VLE of hydrogen mixtures with BIPs from (black lines) this work, (blue lines) [45]

4. Conclusions

Space limitations prevent us from extending this account of recent and ongoing applications of the SOF cohesion function, which also include the correlation of thermodynamic properties of the binary system ammonia-water, for use in the analysis and optimization of refrigeration and power cycles [47–49], and the correlation and prediction of fluid-fluid equilibria of alkyl- and fluoroalkyl-dichlorobenzoates with supercritical carbon dioxide, for use in the selection and design of intermediate compounds in polymer synthesis [50–52]. We believe nonetheless that the above examples provide ample justification for our

conclusion that the SOF cohesion function is a valuable addition to the field of cubic equations of state, and can hold its own against similar tools in current engineering use.

References

[1] J.-M. Yu, Y. Adachi, B. C.-Y. Lu, Selection and design of cubic equations of state, in K. C. Chao, R. L. Robinson Jr. (Eds.), Equations of State. Theories and Applications, ACS Symposium Series 300 (1986) 537–559.

[2] J. D. van der Waals, Over de continuiteit van den gas- en vloeistoftoestand, Doctoral Thesis, University of Leiden, 1873. English translation by J. S. Rowlinson, J. D. Van der Waals: On the continuity of the gaseous and liquid states, Elsevier, Holland, 1988. Spanish translation by J. O. Valderrama, El legado de van der Waals: Su tesis a 100 años del Premio Nobel, Ed. Universidad de La Serena, Chile, 2010.

[3] J. D. van der Waals, Nobel lecture: The equation of state for gases and liquids. Available from: http://www.nobelprize.org/nobel_prizes/physics/laureates/1910/waals-lecture.html.

[4] G. M. Wilson, Vapor-liquid equilibria, correlation by means of a modified Redlich-Kwong equation of state, Advances in Cryogenic Engineering 9 (1964) 168-176.

[5] G. Soave, Equilibrium constants from a modified Redlich-Kwong equation of state, Chemical Engineering Science 27 (1972) 1197-1203.

[6] E. W. Lemmon, M. O. McLinden, D. G. Friend, Thermophysical Properties of Fluid Systems, in P. J. Linstrom, W. G. Mallard (Eds.) NIST Chemistry WebBook, NIST Standard Reference Database Number 69, National Institute of Standards and Technology, Gaithersburg MD. Available from: http://webbook.nist.gov.

[7] C. H. Twu, A modified Redlich-Kwong equation of state for highly polar, supercritical systems, Proceedings of the International Symposium on Thermodynamics in Chemical Engineering and Industry, China, 1988, p. 148-169.

[8] J. H. Vera, J. M. Prausnitz, Interpretative review. Generalized van der Waals theory for dense fluids, Chemical Engineering Journal 3 (1972) 1-13.

[9] S. I. Sandler, The generalized van der Waals partition function. I. Basic theory, Fluid Phase Equilibria 19 (1985) 233-257.

[10] M. M. Abbott, Thirteen ways of looking at the van der Waals equation, Chemical Engineering Progress 85 (1989) 25-37.

[11] D. Henderson, Practical calculations of the equation of state of fluids and fluid mixtures using perturbation theories and related theories, in K. C. Chao, R. L. Robinson Jr. (Eds.), Equations of State in Engineering and Research, ACS Advances in Chemistry Series 182 (1979) 1-30.

[12] W. F. Vogl, K. R. Hall, Generalized temperature dependence of the Redlich-Kwong constants, AIChE Journal 16, 6 (1970) 1103-1104.

[13] J. Mollerup, Thermodynamic properties from a cubic equation of state, SEP 8601, Instituttet for Kemiteknik, Lyngby, Denmark,1986.

[14] R. J. Bakker, Adaptation of the Bowers and Helgeson (1983) equation of state to the H_2O–CO_2–CH_4–N_2–NaCl system, Chemical Geology 154 (1999) 225–236.

[15] R. J. Bakker, Thermodynamic properties and applications of modified van-der-Waals equations of state, Chapter 7 in R. Morales-Rodriguez (Ed.), Thermodynamics – Fundamentals and its Application in Science, InTech, Croatia, 2012.

[16] C. M. Colina, J. W. Santos, C. Olivera-Fuentes, High temperature behaviour of the cohesion parameter of cubic equations of state, High Temperatures–High Pressures 29 (1997) 525-532.

[17] G. Soave, Rigorous and simplified procedures for determining the pure-component parameters in the Redlich-Kwong-Soave equation of state, Chemical Engineering Science 35 (1980) 1725-1729.

[18] A. V. Colazo, F. A. Da Silva, E. A. Müller, C. Olivera-Fuentes, Joule-Thomson inversion curves and the supercritical cohesion parameters of cubic equations of state, Latin American Applied Research 22 (1992) 135-147.

[19] B. I. Lee, M. G. Kesler, A generalized thermodynamic correlation based on three-parameter corresponding states, AIChE Journal 21, 3 (1975) 510-527.

[20] B. Stamateris, C. Olivera-Fuentes, A procedure for the calculation of alpha function coefficients for the attraction parameter of van der Waals equations of state, Proceedings of the 5th World Congress of Chemical Engineering, San Diego, CA, 1996, Vol. I, p. 103-110.

[21] F. Figueira, A. J. Rodríguez, B. C. Stamateris, C. G. Olivera-Fuentes, An energy-based cohesion function for cubic equations of state, Polish Journal of Chemistry 80 (2006) 81-97.

[22] T. E. Daubert, R. P. Danner, Physical and Thermodynamic Properties of Pure Chemicals – Data Compilation. Hemisphere, Washington D. C., 1988.

[23] A. M. Cataño-Barrera, F. L. Figueira, C. Olivera-Fuentes, C. M. Colina, Correlation and prediction of fluid-fluid equilibria of carbon dioxide-aromatics and carbon dioxide-dichlorobenzoates binary mixtures, Fluid Phase Equilibria 311 (2011) 45-53.

[24] J. M. Prausnitz, R. N. Lichtenthaler, E. G. de Azevedo, Termodinámica molecular de los equilibrios de fases, 3rd Ed., Prentice-Hall, Madrid, 2000.

[25] B. E. Poling, J. M. Prausnitz, J. P. O'Connell, The Properties of Gases and Liquids, 5th Ed., McGraw-Hill, New York, 2000.
[26] R. M. Gibbons, A. P. Laughton, An equation of state for polar and non-polar substances and mixtures, Journal of the Chemical Society, Faraday Transactions 2, 80 (1984) 1019–1038.
[27] R. Stryjek, J. H. Vera, PRSV: An improved Peng-Robinson equation of state for pure compounds and mixtures, Canadian Journal of Chemical Engineering 64 (1986) 323-333.
[28] A. J. Rodríguez, M. C. Cuzzi, C. M. Colina, C. Olivera-Fuentes, A generalized Soave-Redlich-Kwong equation of state for polar and nonpolar fluids based on a four-parameter corresponding states principle, Proceedings of the VI Iberoamerican Conference on Phase Equilibria and Fluid Properties for Process Design (CD-ROM), 2002, Document EQ-026.pdf
[29] F. L. Figueira De Barros, Development of equations of state of van der Waals type for polar and nonpolar pire fluids (in Spanish), MSc Thesis, Simón Bolívar University, Caracas, 2005.
[30] F. L. Figueira, L. Lugo, C. Olivera-Fuentes, Generalized parameters of the Stryjek–Vera and Gibbons–Laughton cohesion functions for use with cubic EOS of the van der Waals type, Fluid Phase Equilibria 259 (2007) 105–115.
[31] A. Balliache, S. Kerbage, Temperature dependence of the Redlich-Kwong equation of state for distillation applications (in Spanish), Chemical Engineering Mini-Project, Simón Bolívar University, Caracas, 2003.
[32] O. M. Barrios Viloria, Evaluation of the SOF cohesion function in the prediction of multicomponent vapor-liquid equilibrium (in Spanish), MSc Thesis, Simón Bolívar University, Caracas, 2012.
[33] O. M. Barrios, C. Olivera-Fuentes, F. L. Figueira, Generalized correlation of binary interaction parameters in cubic equations of state for hydrocarbon/CO_2, hydrocarbon/H_2S and CO_2/H_2S systems, Chemical Engineering Transactions 24 (2011) 589-594.
[34] R. Paunović, S. Jovanović, A. Mihajlov, Rapid computation of binary interaction coefficients of an equation of state for vapor-liquid equilibrium calculations. Application to the Redlich-Kwong-Soave equation of state, Fluid Phase Equilibria 6 (1981) 141-148.
[35] R. L. Geddes, Computation of petroleum fractionation, Industrial and Engineering Chemistry 33, 6 (1941) 795-801.
[36] T. E. Daubert, Petroleum fraction distillation conversions, Hydrocarbon Processing 73, 9 (1994) 75-78.
[37] C. H. Twu, An internally consistent correlation for predicting the critical properties and molecular weights of petroleum and coal-tar liquids, Fluid Phase Equilibria 16, 2 (1984) 137-150.
[38] H. Segura, T. Kraska, A. Mejía, J. Wisniak, I. Polishuk, Unnoticed pitfalls os Soave-type alpha functions in cubic equations of state, Industrial and Engineering Chemistry Research 42 (2003) 5662-5673.
[39] R. D. Gunn, P. L. Chueh, J. M. Prausnitz, Inversion temperatures and pressures for cryogenic gases and their mixtures, Cryogenics 6, 6 (1966) 324-329.
[40] Y. Barré, A. V. Colazo, C. Colina, F. A. Da Silva, J. Fuentes, J. W. Santos, E. Silva, C. Olivera-Fuentes, An enthalpy-oriented criterion to determine the supercritical cohesion parameters of cubic equations of state, Paper presented at the Twelfth Symposium on Thermophysical Properties, Boulder, 1994.
[41] J. W. Leachman, R. T. Jacobsen, S. G. Penoncello, E. W. Lemmon, Fundamental equations of state for parahydrogen, normal hydrogen and orthohydrogen, Journal of Physical and Chemical Reference Data 38, 3 (2009) 721-748.
[42] H. M. Bastida Goncalves, Study of the vapor-liquid equilibrium of pure hydrogen and its mixtures using cubic equations of state (in Spanish), BSc Thesis in Chemical Engineering, Simón Bolívar University, Caracas, 2010.
[43] H. M. Bastida, F. L. Figueira, C. Olivera-Fuentes, Modelling vapor-liquid equilibrium of hydrogen and its mixtures by means of equations of state (in Spanish), Paper presented at the Third Congress of Ttheoretical and Computational Physical Chemistry, Caracas, 2010.
[44] P. Englezos, N. Kalogerakis, R. Bishnoi, A systematic approach for the efficient estimation of the interaction parameters in equations of state using binary VLE data, Canadian Journal of Chemical Engineering 71 (2003) 322-326.
[45] M. J. Huron, J. M. Moysan, H. Paradowski, J. Vidal, Prediction of the solubility of hydrogen in hydrocarbon systems through cubic equations of state, Chemical Engineering Science 38 (1983) 1085-1092.
[46] M. Bosse, L. Cisternas, J. Valderrama, M. Vergara, Binary interaction parameters in cubic equations of state for hydrogen-hydrocarbon mixtures, Chemical Engineering Science 45 (1990) 49-54.
[47] F. L. Figueira, C. Olivera-Fuentes, S. Derjani-Bayeh, Calculation of the coefficient of performance of the vapor absorption refrigeration cycle using cubic equations of state, Proceedings of the Eighth Iberoamerican Congress of Mechanical Engineering (CD-ROM), Cusco, 2007, Document 29-18.
[48] F. L. Figueira, S. Derjani-Bayeh, C. Olivera-Fuentes, Prediction of the thermodynamic properties of {ammonia + water} using cubic equations of state with the SOF cohesion function.
[49] S. Derjani-Bayeh, F. L. Figueira, C. Olivera-Fuentes, Representation of thermodynamic properties of {ammonia + water} with cubic equations of state: A statistical analysis, Extended Manuscripts, Ninth Iberoamecian Conference on Phase Equilibria and Fluid Properties for Process Design (ebook), Puerto Varas, 2012, p. 50-72.
[50] A. M. Cataño Barrera, Polymer solutions and solvent-supercritical carbon dioxide studies applying PC-SAFT, MSc Thesis in Materials Science and Engineering, Pennsylvania State University, State Collega, PA, 2011.
[51] A. M. Cataño-Barrera, F. L. Figueira, C. Olivera-Fuentes, C. M. Colina, Correlation and prediction of fluid-fluid equilibria of carbon dioxide-aromatics and carbon dioxide-dichlorobenzoates binary mixtures, Fluid Phase Equilibria 311 (2011) 45-53.

[52] F. L. Figueira, D. Higueras, J. Márquez, A. Parada, C. M. Colina, C. Olivera-Fuentes, Correlation and prediction of fluid phase equilibria in binary {alkyl-dichlorobenzoate + CO_2} and {fluoro-alkyl-dichlorobenzoate + CO_2} systems, Extended Manuscripts, Ninth Iberoamecian Conference on Phase Equilibria and Fluid Properties for Process Design (ebook), Puerto Varas, 2012, p. 80-95.